

Journal of Biomedical Optics

SPIEDigitalLibrary.org/jbo

Visualizing and quantifying difference in cytoplasmic and nuclear metabolism in the hepatobiliary system *in vivo*

Chih-Ju Lin
Ning Kang
Jian-Ye Lee
Hsuan-Shu Lee
Chen-Yuan Dong

Visualizing and quantifying difference in cytoplasmic and nuclear metabolism in the hepatobiliary system *in vivo*

Chih-Ju Lin,^a Ning Kang,^a Jian-Ye Lee,^a Hsuan-Shu Lee,^{b,c,*} and Chen-Yuan Dong^{a,d,e,*}

^aNational Taiwan University, Department of Physics, Taipei 106, Taiwan

^bNational Taiwan University Hospital and National Taiwan University, College of Medicine, Department of Internal Medicine, Taipei 100, Taiwan

^cNational Taiwan University, Institute of Biotechnology, Taipei 106, Taiwan

^dNational Taiwan University, Center for Optoelectronic Biomedicine, Taipei 106, Taiwan

^eNational Taiwan University, Center for Quantum Science and Engineering, Taipei 106, Taiwan

Abstract. The liver is a major organ responsible for performing xenobiotic metabolism. In this process, xenobiotic is uptaken and processed in hepatocytes and subsequently excreted into the bile canaliculi. However, the intracellular heterogeneity in such metabolic processes is not known. We use the molecular probe 6-carboxyfluorescein diacetate (6-CFDA) to investigate xenobiotic metabolism in hepatocytes with intravital multiphoton fluorescence microscopy. 6-CFDA is processed by intracellular esterase to fluorescent 6-CF, which can be imaged and quantified. We found that compared to the nucleus, cytoplasmic 6-CF fluorescence intensity reached a maximum earlier (cytoplasm: 11.3 ± 4.4 min; nucleus: 14.7 ± 4.9 min) following 6-CFDA injection. We also found a slight difference in the rate of 6-CFDA metabolism as the rates of 6-CF decay at rates of 1.43 ± 0.75 and 1.27 ± 0.72 photons/min for the cytoplasm and nucleus, respectively. These results indicate that molecular transport to the nucleus is additionally hindered and can affect drug transport there. © 2015 Society of Photo-Optical Instrumentation Engineers (SPIE) [DOI: 10.1117/1.JBO.20.1.016020]

Keywords: intravital imaging; multiphoton fluorescence microscopy; hepatocyte; hepatobiliary metabolism.

Paper 140711LR received Oct. 30, 2014; accepted for publication Dec. 30, 2014; published online Jan. 22, 2015.

1 Introduction

The liver is the main organ that performs metabolism of unwanted metabolites. Individual hepatocytes would uptake, process, and excrete metabolites into the bile canaculi. However, differences in metabolic kinetics of different organelles are not known. Since the nucleus contains nucleolus, DNA, RNA, and ribosome, it is not expected to be the key component responsible in hepatocellular metabolism. However, the presence of nuclear receptors¹ and their roles in affecting the expression of metabolic enzymes and transporters means that the nucleus mediates signal transduction interactions with cytoplasm and, therefore, can be used as a drug target. In fact, nuclei have been targeted by both drug molecules and nanoparticles for cancer treatment purposes.^{2–4} Therefore, understanding transport dynamics in different cellular compartments *in vivo* may be significant in drug delivery applications.

In previous studies, 6-carboxyfluorescein diacetate (6-CFDA) has been used as a probe for investigating simulate xenobiotic metabolism in the hepatobiliary system. Upon hepatocyte uptake of the neutral 6-CFDA and processing by intracellular esterase, nonfluorescent 6-CFDA is converted into fluorescent 6-CF, which is subsequently excreted into the bile canaculi via the apical (canalicular) membrane.^{5–7} Multidrug resistance associated protein 2 (Mrp2) is the main channel protein responsible in 6-CF excretion.⁸ Therefore, time-lapse fluorescence imaging would allow hepatobiliary dynamics to be studied^{5,6,9} as

6-CFDA was used to investigate changes in hepatobiliary metabolism in acetaminophen induced hepatic necrosis.⁷ In this study, we performed intravital multiphoton microscopy to visualize and quantify differences in 6-CFDA/6-CF metabolism between the cytoplasm and nucleus.

2 Materials and Methods

We used a home-built multiphoton fluorescence microscope in this study. The 780 nm output of a femtosecond, titanium-sapphire (ti-sa) laser (Tsunami, Spectra Physics, Mountain View, CA, USA) pumped by a diode-pump, solid-state laser (Millennia X, Spectra Physics) was used as the excitation source. The ti-sa source was adjusted to be circularly polarized by a quarter waveplate and the power of the laser source was controlled by a combination of a half waveplate and linear polarizer. Subsequently, the laser source was directed into an inverted microscope (Nikon, ECLIPSE TE2000-U, Tokyo, Japan). The ti-sa source was reflected by the main dichroic (700DCSPXRUV-3p, Chroma Technology, Rockingham, VT, USA) into the back aperture of the focusing objective (PlanFlour 20×/NA0.75, oil immersion, Nikon) and the on-sample power was ~80 mW. The excited fluorescence was detected in the epi-illumination geometry, and passed through the main dichroic, secondary dichroic (435DCXR, 495DCXR, 555DCLP, Chroma Technology), and additional band-pass filters (HQ390/20, HQ460/50, HQ525/50, HQ610/75, Chroma Technology) before reaching single-photon

*Address all correspondence to: Hsuan-Shu Lee and Chen-Yuan Dong, E-mail: benlee@ntu.edu.tw and cydong@phys.ntu.edu.tw

counting photomultiplier tubes (R7400P, Hamamatsu, Japan) for detection. In this manner, spectrally resolved images at 380 to 400 nm (second harmonic generation), 435 to 485 nm (blue fluorescence), 500 to 550 nm (green fluorescence), and 550 to 630 nm (red fluorescence) were acquired.

The animals used in this study were seven- to nine-week-old male C57BL/6 mice kept in a 12 h light/12 h dark clock cycle at $23 \pm 1^\circ\text{C}$ and $60 \pm 10\%$ humidity. For intravital imaging, intravital hepatic imaging chambers were installed on the mice as previously described.⁵ Following the installation of the intravital hepatic imaging chamber, the mouse was anesthetized and a catheter (PE-10, Becton Dickinson and Company, NJ, USA) was inserted into the jugular vein for intravenous injection. Rhodamine B isothiocyanate-dextran 70,000 (Sigma, Saint Louis, MO, USA) at the dose of 2.50 mg/mouse [50 mg/ml in phosphate buffered saline (PBS)] was injected to label the hepatic vasculature, and 6-CFDA at the dose of 50 ml (1 mg/ml) in PBS (C1157, Invitrogen, USA) was the probe used for studying hepatocellular metabolism.

With the optical scanning system, the scanned area is limited to $200 \times 200 \mu\text{m}^2$ (x - y mirror scanning system, Model 6220, Cambridge Technology, Lexington, MA). In order to probe the hepatobiliary metabolism over a larger area, a stage scanner (H117, Prior Scientific Inc., Rockland, MA, USA) was used to translate the mouse after each optical scan. In this manner, we were able to acquire a large-area map consisting of 3×3 small-area optical images. In this manner, each 3×3 frame took 1 min to acquire.

3 Results and Discussions

Time-lapse images were acquired over 60 min with time intervals of ~ 1 min. In each mouse, $600 \times 600 \mu\text{m}^2$ images were taken (Fig. 1). 6-CFDA was intravenously injected at the end of the zeroth minute and 6-CF started appearing at the first

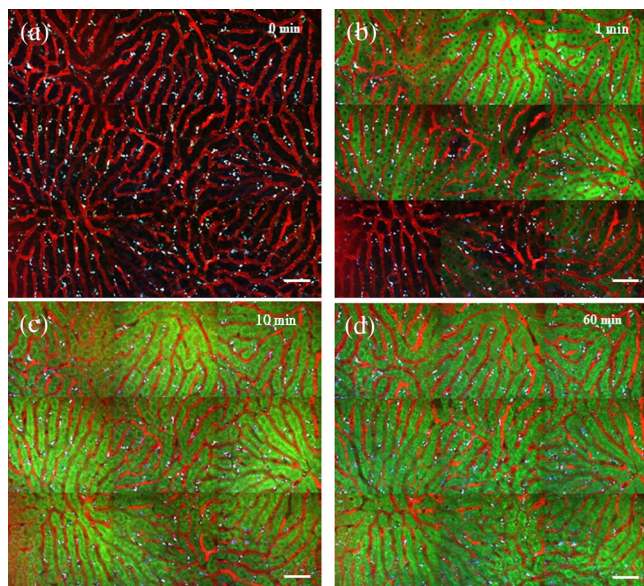


Fig. 1 Time-lapse, intravital multiphoton imaging of hepatobiliary metabolism. Images from four time points following 6-carboxyfluorescein diacetate (6-CFDA) injection were shown (0, 1, 10, and 60 min, with minute 0 as the time point of 6-CFDA injection). Red: rhodamine B isothiocyanate-dextran to label vasculature; green: 6-CF fluorescence; white: hepatic stellate cell. Scale bar was $50 \mu\text{m}$.

minute. As Mrp2 transported 6-CF into the bile duct, the cellular concentration of 6-CF would be decreased with time.

To analyze the temporal dynamics of 6-CF metabolism, the cytoplasm and nucleus of individual hepatocytes were analyzed. As shown in Fig. 2, the cytoplasm and nucleus of a selected hepatocyte (yellow arrow) was calculated, and the 6-CF fluorescence profiles are shown in Fig. 2(g). One metric we used for quantification is the time of maximum fluorescence intensity (TMFI). Qualitatively, 6-CF fluorescence dynamics appear to be different in the cytoplasm and nucleus

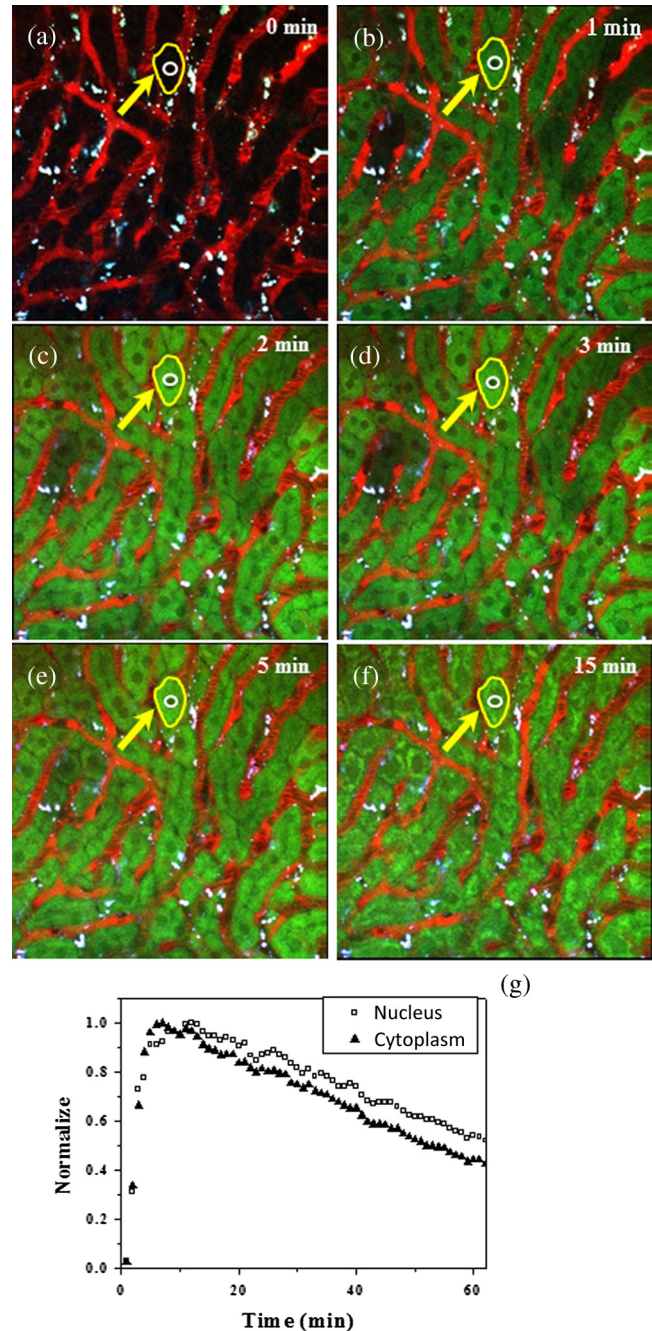


Fig. 2 (a) to (f) show that 6-CF was not present in the nucleus in the first few minutes following 6-CFDA injection. (g) 6-CF fluorescence intensity curve of the enclosed hepatic nucleus and cytoplasm. Scale bar was $50 \mu\text{m}$.

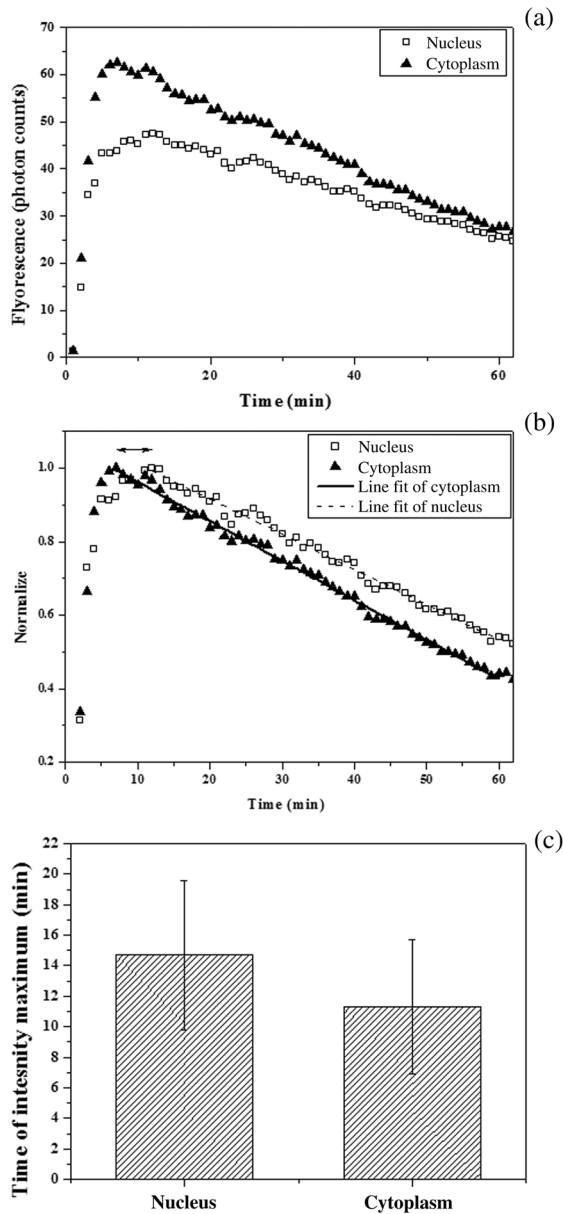


Fig. 3 Hepatocellular fluorescent intensity analysis. (a) Absolute fluorescent intensity of hepatic nucleus and cytoplasm. For the selected hepatocyte, the maximum value of this chosen hepatocyte had ~25% difference between hepatic nucleus and cytoplasm. (b) Normalized hepatic fluorescent intensity showing that metabolism in the nuclei was time-delayed. (c) The time points of maximum fluorescent intensity in hepatic metabolism.

[Figs. 2(a)–2(f)]. Within the first 2 min, 6-CF fluorescence in the cytoplasm was visible; however, there was no fluorescence in the nuclear region. To acquire statistical data, 40 hepatocytes per mouse were randomly selected for analysis of cytoplasmic and nuclear 6-CF fluorescence, and data from five mice were processed.

Detailed analysis of the 6-CF fluorescence decay show additional differences between cytoplasmic and nuclear metabolism (Fig. 3). First, 6-CF fluorescence was more intense in the cytoplasm as the maximum 6-CF fluorescence was higher than that of the hepatic nucleus [Fig. 3(a)]. For all hepatocytes analyzed, the maximum 6-CF fluorescence of the cytoplasmic region was ~7.3% higher than that of the hepatic nucleus. In Fig. 3(b), 6-CF fluorescence was normalized and TMFIs were determined. We found that the peak of 6-CF fluorescence in the cytoplasm is 11.3 ± 4.4 min and that of the nucleus is 14.7 ± 4.9 min (Table 1). Therefore, maximum fluorescence was delayed by 3.4 min for hepatic nuclei. Subsequently, 6-CF fluorescence decreased as 6-CF continued to be excreted into the bile duct. We also linearly fitted 6-CF fluorescence after TMFI and the slopes indicate the relative efficiency of 6-CF metabolism. We found that 6-CF decays at rates of 1.43 ± 0.75 photons/min and 1.27 ± 0.72 photons/min for cytoplasm and the nucleus, respectively. The ratio of the slopes indicates that 6-CFDA metabolism is 5.8% faster in cytoplasm as compared to that of the nuclei.

Differences of cytoplasmic and nuclear metabolism may be attributed to the fact that processed 6-CF needs to pass the nuclear membrane in reaching the nucleus. After 6-CFDA is processed by intracellular esterase, 6-CF would penetrate into the nucleus and eventually be transported out of the nuclear membrane, although at a slower rate than that of cytoplasm.

4 Conclusions

By time-lapse, intravital multiphoton imaging, we found that a difference in xenobiotic metabolism exists between hepatocyte cytoplasm and nucleus. There was a temporal delay in 6-CF reaching the maximum value. A delay of 3.4 min from the nucleus relative to cytoplasm was found. Furthermore, the maximum 6-CF intensity of the cytoplasm was ~7.3% higher than that of hepatic nuclei. In addition, the rate of 6-CF metabolism in the cytoplasm is 5.8% higher than that of the nuclei. This study shows that intravital multiphoton microscopy can be used to visualize and quantify differences in metabolism among different compartments of hepatocytes. The results may be used for the future evaluation of drug delivery efficiency *in vivo*.

Table 1 Summary of the differences between cytoplasmic and nuclear metabolism of 6-carboxyfluorescein diacetate (6-CFDA).

	Time of maximum 6-CF fluorescence intensity (min)	Maximum intensity (photons)	6-CF intensity decay (photons/min)	Slope of normalized 6-CF fluorescence (1/min)
Cytoplasm	11.3 ± 4.4	117.82 ± 44.99	1.43 ± 0.75	0.0120 ± 0.0049
Nucleus	14.7 ± 4.9	109.19 ± 45.69	1.27 ± 0.72	0.0113 ± 0.0037
Cyto-nuc	3.4	8.63	0.16	0.0007
$\frac{ \text{cyto}-\text{Nuc}}{\text{cyto}} \times 100\%$	27.6	7.3	11.2	5.8

Note: Cyto, cytoplasm; nuc, nucleus.

Acknowledgments

We acknowledge the support of the Ministry of Science and Technology (National Science Council) (NSC101-2112-M-002-003-MY3, NSC102-2221-E-002-030-MY3) in Taiwan, National Taiwan University (NTU103R7804), the Center for Quantum Science and Engineering (NTU-ERP-103R891401), and the National Health Research Institute (NHRI-EX102-10041EI).

References

1. Y. Hasegawa et al., "Altered expression of nuclear receptors affects the expression of metabolic enzymes and transporters in a rat model of cholestasis," *Biol. Pharm. Bull.* **32**(12), 2046–2052 (2009).
2. A. L. B. Seynhaeve et al., "Intact doxil is taken up intracellularly and released doxorubicin sequesters in the lysosome: evaluated by in vitro/in vivo live cell imaging," *J. Control. Release* **172**(1), 330–340 (2013).
3. X. J. Zhou et al., "Lactosylated liposomes for targeted delivery of doxorubicin to hepatocellular carcinoma," *Int. J. Nanomed.* **7**, 5465–5474 (2012).
4. N. B. Shah, J. P. Dong, and J. C. Bischof, "Cellular uptake and nanoscale localization of gold nanoparticles in cancer using label-free confocal Raman microscopy," *Mol. Pharm.* **8**(1), 176–184 (2011).
5. F. C. Li et al., "In vivo dynamic metabolic imaging of obstructive cholestasis in mice," *Am. J. Physiol.-Gastroint. Liver Physiol.* **296**(5), G1091–G1097 (2009).
6. Y. Liu et al., "Visualization of hepatobiliary excretory function by intravital multiphoton microscopy," *J. Biomed. Opt.* **12**(1), 5 (2007).
7. F. C. Li et al., "Apical membrane rupture and backward bile flooding in acetaminophen-induced hepatocyte necrosis," *Cell Death Dis.* **2**, e183 (2011).
8. M. Tomita et al., "Suppression of efflux transporters in the intestines of endotoxin-treated rats," *Int. J. Pharm.* **428**(1–2), 33–38 (2012).
9. P. Y. T. Wang et al., "Sex-specific extraction of organic anions by the rat liver," *Life Sci.* **82**(7–8), 436–443 (2008).